J. Fluid Mech. (1970), *vol.* 42, *part* 1, *pp.* 61–83
Printed in Great Britain

Solitary waves in rotating fluids

By W. G. PRITCHARD

Department of Mathematics, The University of Manchester
Institute of Science and Technology†

(Received 10 September 1969)

This paper describes some experiments in rotating flows in which solitary waves were observed.

In one set of experiments the waves were generated on a swirling flow whose circumferential velocity distribution resembled that of the Rankine combined vortex. This flow was established by stirring the liquid in a large cylindrical container, in much the same way as one stirs a cup of tea, and it was often found at the cessation of the stirring that a wave had been generated. This wave propagated along the vortex core and was reflected at the bottom of the container and at the free surface of the liquid and displayed the remarkable permanence characteristic of solitary waves. It appears that, to a first approximation, the speed of the waves may be calculated simply from the depression of the free surface of the liquid at the centre of the vortex. These waves are the rotating-fluid counterpart to the solitary waves in fluids of great depth recently discussed by Benjamin (1967*b*) and by Davis & Acrivos (1967).

In a second set of experiments, solitary waves were generated in a long cylindrical tube and are analogous to the familiar solitary wave of open-channel flows. The theory indicates that these waves are possible in any swirling flow in which the angular velocity is distributed non-uniformly. Thus, a long liquid-filled tube was started rotating about its axis with a uniform angular velocity, and waves were generated before the fluid had reached a state of uniform rotation. Using the known velocity distribution for a tube of infinite length, comparisons have been made between the observed wave forms and the theoretical calculations of Benjamin (1967*a*). There is good agreement between the observed wave forms and the theoretical predictions.

1. Introduction

The present interest in waves of finite amplitude and permanent form arose from the vortex-breakdown phenomenon: this is the abrupt change in structure that sometimes occurs in a swirling flow, particularly in the leading-edge vortex formed above a sweptback lifting surface. An example of the phenomenon, due to Lambourne & Bryer (1962), is reproduced in Batchelor's textbook (1967, plate 22). Among the several attempts to account for the phenomenon theoretically, Benjamin (1962, 1965) proposed that the structural change is a finite transition between two dynamically conjugate states of axisymmetric flow,

† Present address: Department of Chemical Engineering, University of Wisconsin, Madison.

analogous to the undular bore of open channel flow. This theory accordingly indicates the existence of waves of finite amplitude and permanent form in swirling flows, and in a development of the theory Benjamin (1967*a*) has given an approximate analysis of these waves, when bounded by a cylinder, based on the assumption of large wavelengths and wave speeds close to the critical value for infinitesimal waves. The analysis suggests that progressive waves of this type are possible in any swirling flow whose angular velocity is distributed stably and non-uniformly.

A feature of the experimental observations of the phenomenon is the difficulty of preserving the axial symmetry of the motions, as indicated in the photograph of Lambourne & Bryer (1962), or of producing the axisymmetric wave train suggested by the theory. However, in some carefully controlled experiments, Harvey (1962) has come very close to producing a wave train: his experiments showed the first wave of a mild vortex breakdown to be followed by a second one, unless special measures were taken to suppress it, but by the stage of the second wave he found that the motions had become unsteady and irregular. On the other hand, it is possible that such a wave train may be realized more distinctly as a travelling disturbance (the counterpart of the progressive bore) and it was the initial aim of the present experiments to produce this kind of disturbance. It is well known that a body moving slowly along the axis of a *uniformly* rotating fluid pushes an ever-lengthening column of fluid ahead of itself (see Taylor 1922, Benjamin & Barnard 1964), and it was anticipated that the counterpart of the Taylor column, in flows whose angular velocity is distributed non-uniformly, would be analogous to the progressive bore of open channel flows. But, because of limitations of the experimental apparatus, we have been unable to generate this kind of flow and have focused our attention on the limiting form of the bore, the solitary wave. The experiments indicate that the solitary wave may be realized in practice, and its properties are in good agreement with Benjamin's (1967*a*) approximate theory of progressive waves of finite amplitude and permanent form in a cylindrical tube.

A discussion is also given of the long progressive waves of finite amplitude and permanent form that arise in flows of large radial extent. The primary flows on which these waves are manifested have a central core within which the circulation varies significantly and which is surrounded by an extensive region of fluid with constant circulation. The existence of these waves was not unexpected from comparisons with the waves of permanent form in stratified fluids of great depth described by Benjamin (1967*b*) and by Davis & Acrivos (1967); indeed it appears that the present observations of solitary waves arising in fluids of large radial extent are the rotating-fluid counterpart of their internal waves. Waves of this kind are of particular interest since most reports of the vortex breakdown have been made in flows of large radial extent: for example, the photographs of Lambourne & Bryer (1962) already mentioned, and some observations by Maxworthy (1966, 1968) and by Pritchard (1968)† of the breakdown

† The structural change of the flow that occurs in this situation usually takes place very near the stationary surface and there may be some doubt about this interpretation of the change of structure of the flow.

of a jet of fluid ejected from an Ekman layer on a stationary surface are all manifested on a core of strongly rotating fluid surrounded by a vast region of fluid of (essentially) constant circulation. In addition, recent observations by Granger (1968) of surges on a 'bathtub vortex' have a remarkably similar appearance to the initial stages of mild forms of the vortex breakdown.

Benjamin's (1967*b*) theoretical work has shown that the *form* of long waves of finite amplitude is indicated by the 'dispersion relation' between the frequency ω and the wave-number k of infinitesimal periodic waves, for which every dependent variable takes the form

$$u = \hat{u}\, e^{i(\omega t - kx)}, \tag{1.1}$$

where x is the co-ordinate in the direction of propagation and $\hat{u}$ may be a function of the co-ordinate perpendicular to x. For long waves it is sufficient to consider the leading terms of the dispersion relation when expanded as a series for small k. In the customary case of waves of finite amplitude in fluids of finite total depth a good approximation to the phase velocity $W(=\omega/k)$ is, for small enough values of k,

$$W = W_0(1-\beta k^2) \tag{1.2}$$

in which β is a positive constant depending on the particular system under investigation. For these waves the phase velocity has a 'smooth' maximum W_0 at $k = 0$.

However, Benjamin (1967*b*) shows that, for internal waves in fluids of great depth, the leading terms of the dispersion relation for infinitesimal long waves are

$$W = W_0(1-\gamma|k|) \tag{1.3}$$

with $\gamma > 0$, and the phase velocity has a 'sharp' maximum at $k = 0$. The difference between (1.3) and (1.2) has crucial implications on the form of long waves of finite amplitude since it leads to different properties for the two cases with regard to the effective length scale of the waves: Benjamin discusses this point in detail.

Of the two kinds of solitary wave discussed herein, the waves arising in a fluid of large radial extent have leading terms of their dispersion relation of the form

$$W = W_0(1+\beta_1 k^2 \log|k|), \tag{1.4}$$

$\beta_1 > 0$, which we see is again different from (1.2) and (1.3). However, the phase velocity described by (1.4) has a 'smooth' maximum at $k = 0$ and we anticipate that the effective length scale of the solitary waves will be determined by similar considerations to those employed in the customary case, but we have been unable to find the solution to the resulting solitary-wave equation. The dispersion relation for waves generated in a long cylindrical tube has leading terms of the form indicated in equation (1.2), and accordingly the solitary wave in this case is analogous to the customary solitary wave (see Benjamin 1967*a*).

In the first half of the paper these theoretical aspects are discussed in relation to the experiments to follow. Then in the latter half of the paper the experimental observations of the solitary waves are described and compared with the theories. For the motions in a fluid of large radial extent the critical speed of extremely long infinitesimal waves has been found, for a nearly realistic model, and this

speed agrees fairly well with the speeds of the observed wave forms. The experiments concerning solitary waves in a tube are compared with the theory as follows. A long liquid-filled tube, initially at rest, was suddenly set rotating about its own axis with a uniform angular velocity, and before the liquid had attained a state of rigid-body rotation the wave was generated. Knowing the distribution of circumferential velocity we can, for this experiment, give a theoretical estimate of the critical speed and from measurements of the actual wave speed we deduce the amplitude and shape of the solitary wave (Benjamin 1967*a*). These are found to be in fairly good agreement with the observed wave form.

2. The governing equations

The motions are described in terms of the stream function $\psi = \psi(r, x)$ in which r and x denote the radial and axial co-ordinates, with x increasing in the direction of the flow. It is convenient to introduce $y = \frac{1}{2}r^2$, so that

$$\partial/\partial y = r^{-1}(\partial/\partial r).$$

The waves are assumed to arise on a primary, cylindrical state of flow in which the axial velocity W and the swirl velocity V are prescribed functions of y alone. Therefore, the stream function Ψ for the primary flow is defined by $W = d\Psi/dy$, $\Psi(0) = 0$. Accordingly the stagnation pressure $\rho H = p + \frac{1}{2}\rho(W^2 + V^2)$ and the quantity $I = yV^2$, which is $(1/8\pi^2)$ times the square of the circulation, are both functions of y or of Ψ. For an axisymmetric flow arising from this primary state without energy losses, the stream function $\psi(y, x)$ satisfies the equation (see Fraenkel 1956, or Benjamin 1962)

$$\psi_{yy} + \frac{1}{2y}\psi_{xx} = H'(\psi) - \frac{1}{2y}I'(\psi). \tag{2.1}$$

It is convenient to transform (2.1) to an equation for $y = y(x, \psi)$, where y represents the distance of the stream surface ψ from the axis. Under this transformation the radial and axial components of the velocity are

$$u = \frac{1}{\sqrt{(2y)}}\frac{y_x}{y_\psi}, \quad w = \frac{1}{y_\psi}, \tag{2.2}$$

and the governing equation (2.1) becomes

$$\frac{y_{\psi\psi}}{y_\psi^3} + \frac{1}{2y}\left(\frac{y_{xx}}{y_\psi} - \frac{2y_x y_{x\psi}}{y_\psi^2} + \frac{y_x^2 y_{\psi\psi}}{y_\psi^3}\right) = -\left(H'(\psi) - \frac{1}{2y}I'(\psi)\right). \tag{2.3}$$

In this study we are interested in waves that travel at constant speeds and these can be made stationary on a flow of uniform velocity W. Hence in the undisturbed primary flow, we see for constant W that y has the value ψ/W, and accordingly (2.3) is readily expressed as an equation for $y = y(x, \eta)$ where $\eta = \psi/W$.

3. Infinitesimal sinusoidal waves

Initially we consider a fluid that has a large radial extent, and we assume the existence of a region $y \leqslant \alpha$ near the axis, within which the circulation varies significantly and outside which the circulation is a constant. The idea is illustrated in figure 1 where the flow field is defined by regions I and II respectively. Then, to determine the motions within a cylindrical tube, we consider a solid boundary to exist at $y = \alpha$ and we use the boundary conditions applicable to this new situation.

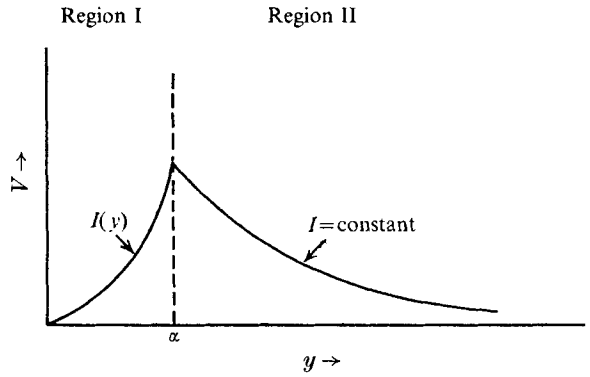

FIGURE 1. Definition sketch showing the circumferential velocity distribution.

Approximate solutions of equation (2.3), written in terms of η, may be found by putting

$$y - \eta = \epsilon\zeta(x, \eta) \tag{3.1}$$

and expanding in powers of ϵ. The zeroth-order solution is $H'(\eta) = (1/2\eta)I'(\eta)$, which implies that $(1/\rho)\,dp/d\eta = V^2/2\eta$.

At the first order in ϵ we find, in the outer region, that both $I'(\eta)$ and $H'(\eta)$ vanish, and hence the linearized equation is

$$\zeta_{\eta\eta} + \frac{1}{2\eta}\zeta_{xx} = 0. \tag{3.2}$$

The boundary conditions imposed on ζ in the outer region are that $\zeta \to 0$ as $\eta \to \infty$ and that ζ takes the value $\zeta(\alpha)$ at $y = \alpha$. A solution of equation (3.2) of the form $\zeta = \phi(\eta)\,e^{ikx}$, k real, satisfying the boundary conditions is

$$\phi = A\sqrt{\eta}\,K_1(|k|\sqrt{(2\eta)}), \quad \text{for} \quad \eta \geqslant \alpha, \tag{3.3}$$

where K_1 is the modified Bessel function of the second kind of order one. A is a constant determined at $\eta = \alpha$.

In region I the linearized equation is

$$\zeta_{\eta\eta} + \frac{I_\eta}{2W^2\eta^2}\zeta + \frac{1}{2\eta}\zeta_{xx} = 0, \tag{3.4}$$

and, for solutions of the form $\zeta = \phi(\eta)\,e^{ikx}$, the appropriate boundary conditions are

$$\left.\begin{aligned} \phi(0) &= 0, \\ \phi, \phi' \quad &\text{continuous across } \eta = \alpha. \end{aligned}\right\} \tag{3.5}$$

Equation (3.4) coupled with (3.5) and (3.3) determines a set of eigenvalues $W^{(n)}$ for a given k. The largest value, $W^{(0)}$, is the critical speed of infinitesimal waves, and has a maximum at $k = 0$. Benjamin (1967*b*) has shown that the way $W^{(0)}$ approaches its maximum at $k = 0$ greatly influences the form of long waves of finite amplitude: for example, Benjamin shows that the length scale of the conventional solitary wave of open-channel flow is quite different from that of the internal solitary wave in fluids of great depth, a consequence of the different forms of $W^{(0)}$ in the two cases. Thus we examine the form of the dispersion relation near $k = 0$ for the two situations of interest in this investigation.

3.1. *Infinitesimal waves in a fluid of large radial extent*

We assume that the primary flow has the same distribution of circumferential velocity as that of the Rankine vortex. Thus the swirl velocity is given by

$$\left.\begin{aligned} &\text{Region I} \quad (y \leqslant \alpha)\text{: } V = \Omega r, \qquad I = 2\Omega^2 y^2, \\ &\text{Region II} \quad (y \geqslant \alpha)\text{: } V = 2\Omega\alpha/r, \quad I = 2\Omega^2\alpha^2. \end{aligned}\right\} \tag{3.6}$$

An approximate solution in region II is given by equation (3.3). The motions in region I, for small sinusoidal disturbances, are found from (3.4) which becomes

$$\phi_{\eta\eta} + (\Gamma^2/\eta)\phi = 0, \tag{3.7}$$

where

$$\Gamma^2 = (2\Omega^2/W^2 - k^2/2).$$

The solution of (3.7) satisfying the condition $\phi(0) = 0$ is (for $\Gamma^2 > 0$)

$$\phi = B\sqrt{\eta}\, J_1(2|\Gamma|\sqrt{\eta}) \quad (\eta \leqslant \alpha), \tag{3.8}$$

and J_1 is the first-order Bessel function of the first kind.

The condition that ϕ is continuous across $\eta = \alpha$ determines the ratio of the constants A and B of (3.3) and (3.8). Therefore, the requirement that ϕ' is continuous across $\eta = \alpha$ constitutes an eigenvalue problem for W, and we find that W is determined by

$$\frac{J_0(2|\Gamma|\sqrt{\alpha})}{J_1(2|\Gamma|\sqrt{\alpha})} = -\frac{1}{\sqrt{2}}\frac{|k|}{|\Gamma|}\frac{K_0(|k|\sqrt{(2\alpha)})}{K_1(|k|\sqrt{(2\alpha)})}, \tag{3.9}$$

and K_0, K_1 are the zero and first-order modified Bessel functions of the second kind.

When k is small the right-hand side of (3.9) is small, and hence its solutions are near the zeros of $J_0(2|\Gamma|\sqrt{\alpha})$. Expanding $J_0(2|\Gamma|\sqrt{\alpha})$ in a Taylor series about its zeros we find that the eigenvalues are given approximately, for small k, by

$$2|\Gamma|\sqrt{\alpha} - j_{0,n} = -\frac{k^2\sqrt{\alpha}}{|\Gamma|}\{\log(|k|\sqrt{(\alpha/2)}) + \gamma\}, \tag{3.10}$$

where $j_{0,n}$ is the nth zero of J_0 and γ is Euler's constant. Restricting our attention to the first eigenvalue we see that (3.10) implies a dispersion relation of the form

$$W = W_0\{1 + \beta_1 k^2 \log|k| + \ldots\}, \tag{1.4}$$

where β_1 is positive and W_0, the critical speed for long waves, is

$$W_0 = \frac{2\Omega\sqrt{(2\alpha)}}{j_{0,1}}. \tag{3.11}$$

3.2. *The critical speed for the experiment in a fluid of large radial extent*

We see from (3.11) that the critical speed of infinitesimal waves propagating along a Rankine vortex is determined by two parameters Ω and α. Anticipating the experiments, it is interesting to note that, if this vortex is generated in a body of fluid having a free surface, the critical speed can be calculated from the depression of the free surface at the centre of the vortex. To see this we denote by z the height of the surface of the liquid above its level at the axis of rotation, and let $z \to z_0$ at large radii. Thus z may be described as a function of the pressure (p) in the liquid and is given by

$$gz = \int_0^r \frac{1}{\rho}\frac{dp}{dr}\,dr, \tag{3.12}$$

where g is the acceleration due to gravity and ρ is the density of the liquid. But (3.12) may be expressed in terms of the circumferential velocity (V), and introducing $y = \frac{1}{2}r^2$ we find that

$$gz = \frac{1}{2}\int_0^y \frac{V^2}{y}\,dy. \tag{3.13}$$

Hence the circumferential velocity distribution may be represented by a new parameter, $\xi(= z/z_0)$, and for extremely long sinusoidal waves ($k = 0$) we find that, in terms of ξ, (3.4) becomes

$$\phi_{yy} + n\{2\xi'/y + \xi''\}\phi = 0, \tag{3.14a}$$

where $n = gz_0/W^2$. If the velocity $V \sim (1/r)$ as $r \to \infty$ the boundary conditions are (cf. Benjamin 1967*b*, § 5)

$$\left.\begin{aligned} \phi(0) &= 0, \\ \phi'(y) &\to 0 \quad \text{as} \quad y \to \infty. \end{aligned}\right\} \tag{3.14b}$$

As indicated above, this system of equations determines a set of eigenvalues the largest of which is termed the critical speed.

Using the velocity distribution of the Rankine vortex (equation (3.6)) we find that (3.14) becomes

$$\left.\begin{aligned} &\phi_{yy} + (n/\alpha y)\phi = 0, \\ &\phi(0) = 0, \quad \phi'(\alpha) = 0. \end{aligned}\right\} \tag{3.15}$$

The solution of the system (3.15) is of the same form as that given in (3.8) and the boundary conditions require that the first mode has $n = \frac{1}{4}j_{0,1}^2 = 1{\cdot}446$. Hence the critical speed for infinitesimal waves is, in this case,

$$W_0 = \sqrt{(gz_0)}/1{\cdot}202, \tag{3.16}$$

which is simply related to the depression of the free surface of the liquid at the centre of the vortex, as anticipated above.

However, when V has more realistic forms it is not so easy to solve (3.14) and find n. But a good approximation to the first mode may be found in any specific case by the Rayleigh method of approximating eigenvalues. The system (3.14) is

equivalent to the variational principle that ϕ should give a minimum value of n according to

$$n = \frac{\int_0^\infty \phi_y^2 \, dy}{\int_0^\infty (\xi'' + 2\xi'/y)\,\phi^2 \, dy}. \tag{3.17}$$

The basis of the Rayleigh method is that an *approximation* to $\phi(y)$, satisfying the boundary conditions, gives an upper bound to the smallest eigenvalue when substituted in (3.14), and this upper bound is often a good estimate of n. The estimate is made more accurate when ϕ is chosen to depend on parameters which are varied to make n a minimum.

As an example we approximate the system (3.15) by the function

$$\phi = \sin(\pi y/2\alpha). \tag{3.18}$$

The estimate of n from (3.17) is $n = 1{\cdot}50$, which is fairly close to the correct answer $1{\cdot}446$.

When ϕ is chosen with a free parameter, which may be varied to minimize n, a better estimate is obtained. For example, if we choose

$$\phi = x - \tfrac{1}{2}\lambda x^2 - \tfrac{1}{3}(1-\lambda)x^3 \quad (x = y/\alpha) \tag{3.19}$$

the expression (3.17) for n becomes

$$n = \frac{\frac{8}{15} - \frac{7}{32}\lambda + \frac{1}{30}\lambda^2}{\frac{19}{54} - \frac{37}{270}\lambda + \frac{31}{2160}\lambda^2} \tag{3.20}$$

and the minimum value, found by varying λ, is $n = 1{\cdot}447$. The correct answer for n is $1{\cdot}446$ so the method appears to work fairly well in this case. Thus, having checked the method, we proceed to a more realistic velocity distribution and use it to estimate the critical speed.

A better representation of the velocity distribution (see figure 3 to follow) is given by the Burgers vortex,

$$V^2 = (D/y)(1 - e^{-\kappa y})^2, \tag{3.21}$$

where D and κ are constants. With a swirl velocity of this form, the system (3.14) becomes

$$\left.\begin{aligned} &\phi_{yy} + \frac{n}{\log 2}\left\{\frac{e^{-\kappa y}(1-e^{-\kappa y})}{y^2}\right\}\phi = 0, \\ &\phi(0) = 0, \quad \phi'(y) \to 0 \quad \text{as} \quad y \to \infty, \end{aligned}\right\} \tag{3.22}$$

and the smallest eigenvalue gives the critical speed of infinitesimal waves. To estimate this eigenvalue by the Rayleigh method we choose

$$\phi = 1 - e^{-\Lambda y}, \tag{3.23}$$

which satisfies the boundary conditions with any $\Lambda > 0$. In this case the estimate of n according to (3.17) is

$$n = \frac{\log 2}{2}\left\{\begin{matrix} (\lambda+2)\log(\lambda+2) + \lambda\log\lambda - 2(\lambda+1)\log(\lambda+1) \\ -2(\lambda+1)\log 2(\lambda+1) + 2\lambda\log 2\lambda + 2(2\lambda+1)\log(2\lambda+1) \end{matrix}\right\}^{-1}, \tag{3.24}$$

where λ has been written for κ/Λ. The minimum value of n, which is found by maximizing the bracketed term of (3.24) is 1·691. Hence the critical speed of infinitesimal waves is

$$W_0 = \sqrt{(gz_0)}/1{\cdot}30. \tag{3.25}$$

An interesting feature of the analysis is that, as in the previous example, the estimate of n is independent of the cross-sectional dimension, κ, of the vortex, and the critical speed is again given in terms of the depression of the surface of the liquid at the centre of the vortex.

3.3. *Infinitesimal waves in a bounded fluid*

It was anticipated in the introduction that waves of finite amplitude and permanent form progressing along a cylindrical tube would be analogous to the familiar finite-amplitude waves of open channel flow. Accordingly the dispersion relation has a 'smooth' maximum near $k = 0$, and to illustrate this it is sufficient to consider a uniformly rotating fluid within a cylinder whose radius is given by $y = \alpha$. The motions are governed by equation (3.7) with the boundary condition at $\eta = \alpha$ given by $\phi(\alpha) = 0$. The solution is given in (3.8), and the condition $\phi(\alpha) = 0$ determines a set of eigenvalues given by

$$2\,|\Gamma|\sqrt{\alpha} = j_{1,n} \tag{3.26}$$

where $j_{1,n}$ is the nth zero of J_1.

Thus, we see that the dispersion relation is of the form

$$W = W_0(1 - \beta k^2 + \ldots), \tag{1.2}$$

where $\beta > 0$, and $W_0 = 2\Omega\sqrt{(2\alpha)}/j_{1,n}$.

3.4. *The critical speed for the experiments in a bounded fluid*

The theory (§ 4 and see Benjamin 1967*a*) indicates that the solitary wave does not exist in a long cylindrical tube if the primary flow is one of uniform angular velocity, and recent experiments (Pritchard 1969) confirm this prediction. The experiments suggest that, in a uniformly rotating fluid, no (finite amplitude) disturbances are propagated at speeds in excess of the critical speed, thereby precluding the possibility of waves of finite amplitude and permanent form. Thus, to realize the solitary wave in a long tube we require a non-uniform (and stable) distribution of circumferential velocity. This has been accomplished in the present experiments by generating the wave before the fluid in the tube, in response to suddenly starting the tube rotating, has had time to reach rigid-body rotation; for sufficiently large wave speeds the velocity distribution changes by a negligible amount during the time of passage of the wave along the tube.

In an infinitely long tube of radius b, containing fluid initially at rest, an exact description of the velocity distribution is known at any instant after the tube begins rotating about its axis with a uniform angular velocity, Ω. Thus, after a time t, the circumferential velocity at a radius r is (see Batchelor 1967, p. 203)

$$V(r,t) = \Omega r + 2\Omega b \sum_{n=1}^{\infty} \left\{ \frac{J_1(j_n r/b)}{j_n J_0(j_n)} \exp\left(-j_n^2 \frac{\nu t}{b^2} \right) \right\}, \tag{3.27}$$

where j_n is the nth zero of J_1. The velocity distribution, V, is shown in figure 2 at various stages of the development of the flow.

This velocity distribution is nearly realized in the laboratory in a very long tube. The difference between the laboratory experiment and the theoretical distribution arises because of the finite length of the tube, but it appears that, in a long tube, the ends have a fairly small effect on the initial flow.† To check this some measurements of the circumferential velocity were made during the spinning-up process by taking ciné photographs of small (approximately 1 mm

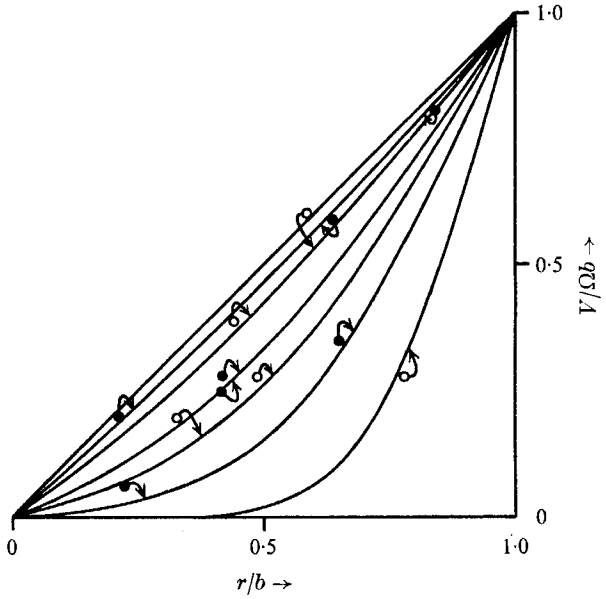

FIGURE 2. The velocity distribution in an infinitely long tube started rotating about its own axis at $t = 0$. The curves correspond to the following values of tv/b^2 (increasing outwards): 0·020; 0·050; 0·075; 0·100; 0·150; 0·200. The velocity everywhere differs by less than 0·01 % from that of rigid-body rotation for values of $tv/b^2 \geqslant 1{\cdot}0$.

diameter) neutrally buoyant particles suspended in the liquid. The results of these measurements are given in figure 2, and although the results are subject to a fairly large error it appears that the theoretical distribution (3.27) is a good description of the circumferential velocities in the experimental apparatus.

Hence the theoretical velocity distribution (3.27) can be used with a high degree of confidence to calculate, at any instant, the critical speed of infinitesimal waves in the tube. This speed is found from the smallest eigenvalue (for extremely long waves) of (3.4), taken with the boundary conditions $\zeta(0) = 0$, $\zeta(\alpha) = 0$ (or see (4.11) to follow). Because of the complicated expression for V the eigenvalues

† In these experiments the upper surface of the water was free and a layer about one tube diameter in depth, of a more dense liquid (carbon tetrachloride), was placed in the bottom of the tube. It is thought that this layer of carbon tetrachloride considerably reduced the meridional flow in the tube, but no quantitative measurements were made to check this.

have been found numerically. The system of equations was represented by its first-order finite differences and the eigenvalues of this representation were found. The computations suggested that this method of solution gave the desired results: the solutions appeared to converge very rapidly towards a limit as more and more accurate representations of the equations were taken, and the answers agree to a very high accuracy with the analytic solution for the case of a uniform angular velocity distribution ($t \to \infty$). The results of these computations are given in figure 9, to follow.

4. Long waves of finite amplitude

4.1. *The solitary wave in a fluid of large radial extent*

It is assumed that the solitary wave arises on a primary flow having the same distribution of circumferential velocity as that of the Rankine vortex described in the infinitesimal wave theory (see equation (3.6)). To find an approximation to stationary waves of finite amplitude we must develop at least two stages of an asymptotic expansion in terms of a small parameter ϵ, measuring amplitude. Thus, we write

$$y - \eta = \epsilon\zeta = \epsilon\zeta_0(X, \eta) + \epsilon^2\zeta_1(X, \eta) + \ldots, \tag{4.1}$$

where X represents a 'stretched' axial co-ordinate such that derivatives with respect to X are of the same order of magnitude as the functions differentiated. Guided by the considerations outlined in the introduction we specify

$$X = \epsilon^{\frac{1}{2}}x \tag{4.2}$$

for a system having a dispersion relation with leading terms of the form (1.4).

The wave speed W is also represented by a series expansion, and hence we put

$$W^2 = W_0^2(1 + \epsilon\Delta_1 + \ldots), \tag{4.3}$$

where W_0 is the 'critical' speed for infinitesimal waves, as given by (3.11).

The solution in region II follows the same arguments as described in the linearized theory. In terms of the scaled co-ordinates the governing equation for region II is

$$\zeta_{\eta\eta} + \frac{\epsilon}{2\eta}\zeta_{XX} = 0 \quad (\eta \geqslant \alpha). \tag{4.4}$$

To find approximate solutions for long waves of arbitrary shapes we assume ζ may be denoted by

$$\left.\begin{aligned} \zeta(X, \eta) &= F(X)\,\phi(\eta) \\ \text{with} \quad \zeta(X, \alpha) &= F(X). \end{aligned}\right\} \tag{4.5}$$

For a solitary wave, $F(X)$ may be expressed in terms of a Fourier integral with transform $\tilde{F}(K)$ where

$$\tilde{F}(K) = \frac{1}{2\pi}\int_0^\infty F(X)\exp[iKX]\,dX. \tag{4.6}$$

Then the solution of (4.4), of the form (4.5) and which vanishes for $\eta \to \infty$, is

$$\zeta(X, \eta) = \int_{-\infty}^{\infty} \tilde{F}(K)\,e^{-iKX}\sqrt{(\eta/\alpha)}\,\frac{K_1[\epsilon^{\frac{1}{2}}|K|\sqrt{(2\eta)}]}{K_1[\epsilon^{\frac{1}{2}}|K|\sqrt{(2\alpha)}]}\,dK. \tag{4.7}$$

In order to match the solutions for the inner and outer regions we require that $\zeta_\eta(X,\eta)$ is continuous across $\eta=\alpha$. It follows from (4.7) that

$$\zeta_\eta(X,\alpha) = -\epsilon^{\frac{1}{2}}\int_{-\infty}^{\infty} \tilde{F}(K)\, e^{-iKX}\, \frac{|K|}{\sqrt{(2\alpha)}}\, \frac{K_0[\epsilon^{\frac{1}{2}}|K|\sqrt{(2\alpha)}]}{K_1[\epsilon^{\frac{1}{2}}|K|\sqrt{(2\alpha)}]}\, dK. \tag{4.8}$$

Since the theory is based on long waves it is assumed that $\tilde{F}(K)\to 0$ sufficiently rapidly, as $|K|$ increases, that we may use the well-known approximations to the Bessel functions for small K; thus we find that

$$\zeta_\eta(X,\alpha) = -\epsilon\mathscr{F}\{F(X)\}, \tag{4.9}$$

where $\mathscr{F}\{F(X)\}$ is approximately given by

$$\mathscr{F}\{F(X)\} = \int_{-\infty}^{\infty} -K^2\log|K|\,\tilde{F}(K)\,e^{-iKX}\,dK. \tag{4.10}$$

Having determined the outer boundary condition for region I we may now proceed with the solution in that region. The first approximation to equation (2.3) follows the linearized theory (cf. (3.7)) and is given by

$$\zeta_{0\eta\eta} + \frac{I'(\eta)}{2W_0^2\eta^2}\,\zeta_0 = 0 \quad (\eta \leqslant \alpha), \tag{4.11a}$$

with the boundary conditions

$$\left.\begin{aligned}\zeta_0(X,0) &= 0,\\ \zeta_{0\eta}(X,\alpha) &= 0.\end{aligned}\right\} \tag{4.11b}$$

For long waves we assume the solution of (4.11) may be written in the form

$$\zeta_0 = F(X)\,\phi_0(\eta), \tag{4.12}$$

$\phi_0(\alpha)=1$, so that a second approximation to (2.4) is

$$\zeta_{1\eta\eta} + \frac{I'(\eta)}{2W_0^2\eta^2}\,\zeta_1 = \frac{I'(\eta)}{2W_0^2\eta^2}\{F^2(\phi_0^2/\eta - 3\phi_0\phi_{0\eta}) + \Delta_1\phi_0 F\} - \frac{1}{2\eta}\,\phi_0 F_{XX}$$

$$= R(\eta), \quad \text{say.} \tag{4.13a}$$

The outer boundary condition, determined from region II, is given by (4.9). Thus the boundary conditions on (4.13a) are

$$\left.\begin{aligned}\zeta_1(X,0) &= 0,\\ \zeta_{1\eta}(X,\alpha) &= -\mathscr{F}\{F(X)\}.\end{aligned}\right\} \tag{4.13b}$$

Only the particular integral of (4.13a) is needed and it is

$$\zeta_1 = \phi_0\int_0^\eta \frac{1}{\phi_0^2}\int_0^{\eta'} \phi_0 R(\eta'')\,d\eta''\,d\eta'. \tag{4.14}$$

Then for (4.14) to satisfy the boundary conditions (4.13*b*), we must have

$$\left.\begin{aligned} & AF_{XX}+BF^2+CF = \mathscr{F}\{F\}, \\ \text{where} \quad & A = \int_0^\alpha \phi_0^2/2\eta\, d\eta, \\ & B = \int_0^\alpha \{3\phi_0^2\phi_{0\eta}-\phi_0^3/\eta\}\,\frac{I'(\eta)}{2W_0^2\eta^2}\,d\eta, \\ & C = -\Delta_1\int_0^\alpha \phi_0^2\,\frac{I'(\eta)}{2W_0^2\eta^2}\,d\eta. \end{aligned}\right\} \tag{4.15}$$

The solution of (4.15), with $\mathscr{F}\{F\}$ determined by (4.10), gives the approximate form of the solitary wave. Although the explicit solution of this equation is not known, Dr T. B. Benjamin has indicated in recent correspondence that it in fact belongs to a class of equations for which he has been able to prove the existence of a solitary-wave solution.

4.2. *The solitary wave in a radially bounded fluid*

The analysis proceeds in a similar way to that above, except that the flow domain is restricted to region I and that the outer boundary condition for region I is (because of the tube wall at $\eta = \alpha$) one of no radial displacement so that $\zeta(X,\alpha) = 0$. Moreover, the preceding discussion on the effective length of the wave suggests that we once again use a scaled axial co-ordinate X, given by $X = \epsilon^{\frac{1}{2}}x$.

Thus a first approximation to (2.3) is again given by (4.11*a*) but the solution is subject to the new outer boundary condition of $\zeta_0(X,\alpha) = 0$.

The second approximation (of the form $\zeta_0 = F(X)\,\phi_0(\eta)$) is again given by the integral (4.14), but the outer boundary condition $\zeta_1(X,\alpha) = 0$ requires that

$$\int_0^\alpha \phi_0 R(\eta)\,d\eta = 0. \tag{4.16}$$

This may be written as $$AF_{XX}+BF^2+CF = 0 \tag{4.17}$$

with A, B and C the same as given in (4.15). Equation (4.17) was first derived by Benjamin (1967*a*) and has the solution

$$F = -\tfrac{3}{2}(C/B)\,\mathrm{sech}^2\{-\tfrac{1}{2}(C/A)\,X\}. \tag{4.18}$$

An important consequence of Benjamin's solution arises when $V = \Omega r$: the coefficient B vanishes and hence the solitary wave does not exist when the flow is one of rigid-body rotation.

5. Experiments in a fluid of large radial extent

To simplify the analysis it has been assumed that the solitary wave arises on a primary flow described by the Rankine combined vortex (see (3.6)). Although this flow cannot be established in practice a real vortex exhibits the major characteristics of the Rankine vortex and the analysis can, in principle, be extended

to cover more realistic distributions of the circumferential velocity (Benjamin 1967*b* discusses this point in greater detail).

Turner (1966) has measured the swirl-velocity profile in a laboratory model of a tornado vortex and found it to have a uniformly rotating central core surrounded by a large expanse of fluid with a constant circulation, the two regions being connected by a smooth transition, as opposed to the sharp boundary in the Rankine vortex. Velocity profiles similar to those measured by Turner have been found in the present experiments and it appears that the results may be fairly well represented by the Burgers vortex (see (3.21)).

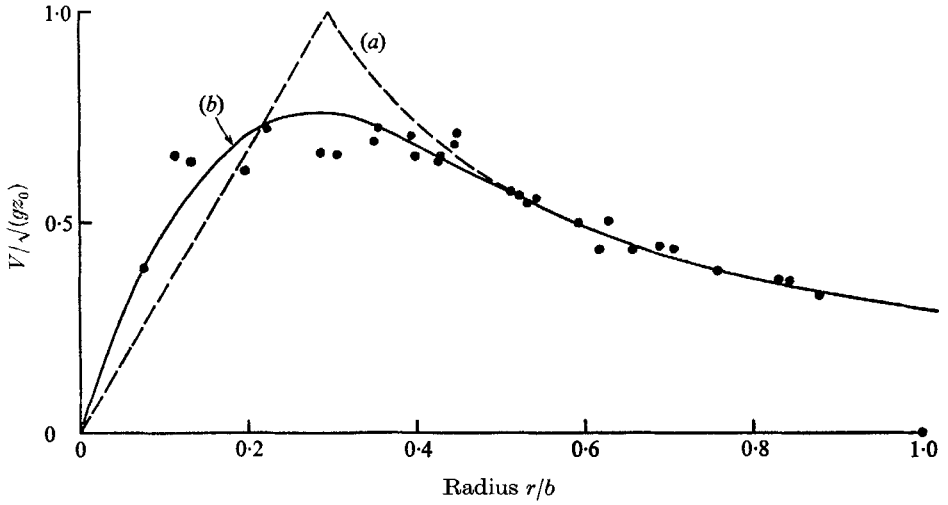

FIGURE 3. The circumferential velocity distribution after stirring a liquid in a cylindrical container of radius b. The parameters were determined from the measured velocity at $r/b = 0{\cdot}6$ and from an independent measurement of z_0 (the depression of the free surface at $r/b = 0$). (*a*) $V = \Omega r$ for $0 \leqslant r \leqslant R$, $V = \Omega R^2/r$ for $R \leqslant r < \infty$. (*b*) $V = \sqrt{2}(D/r)(1 - e^{\kappa r^2/2})$.

The present experiments were carried out in a large Perspex cylinder (30·5 cm diameter and 61 cm in length) filled with water. The liquid in the cylinder was stirred, in much the same way as one stirs a cup of tea, with a 1 cm-diameter rod, the resultant Ekman layer on the bottom of the container causing a concentration of vorticity at the centre of the cylinder. To see how closely this flow was represented by the vortex models some measurements were made of the circumferential velocity distribution. These measurements were made at the surface of the liquid from streak photographs of slightly buoyant spheres of about 1 mm diameter. Since most of the volume of any sphere was below the surface and since the surface film had been removed with a suction hose immediately preceding each experiment, it was thought that this measurement should give a good estimate of the swirl velocity. The results of a measurement of this kind are shown in figure 3 and the data is compared with the two vortex models. Both these models are characterized by two parameters, and hence two independent measurements of the flow are needed to specify them. A typical value of the

circumferential velocity was chosen from the measurements in the region of constant circulation which, together with a measurement of the depression of the free surface at the centre of the vortex, is sufficient information to specify the models. Thus the velocity data has been 'fitted' to the models at only one point and yet the models represent the measured velocities fairly well at all radii.

Thus a swirling flow was established in the Perspex cylinder by stirring the liquid with a rod. When the desired amount of circulation had been generated in the water the stirring was stopped and the fluid motions investigated by introducing a small amount of coloured water to the centre of the vortex.† On most occasions the motions of the dyed liquid indicated a wave propagating along the axis, being reflected at the surface and at the bottom. It is thought that this wave is generated during the stirring procedure. Alternately, if a wave is not generated in this manner one may be generated independently by plunging a rod (a rod of about 3 cm diameter worked well in this case) a short distance along the axis and then withdrawing it. The experiment is quite spectacular, particularly when dye is introduced at the surface, because the dye forms into a series of mantles and the large displacements that occur in the core of the vortex are easily seen.

By introducing dyed water at various positions along the axis it was easy to follow the passage of the wave along the vortex core, from the top to the bottom of the container and back again. It was evident that a fluid particle in the core was given a net axial displacement as the wave passed, a characteristic feature of the solitary wave. However, the striking feature of the motion is the remarkable persistence shown by the wave: the wave could clearly be observed for several minutes, in which time it travelled many hundreds of core diameters.

Some measurements of the wave speed have been made to see how closely it corresponds to the theoretical estimates of the critical speed of infinitesimal waves described in § 3.2. One set of results was obtained by measuring, with a stop watch, the time for the wave to travel from the surface, to the bottom of the container, and back to the surface. A more accurate set of results was obtained from ciné photographs of the elevation of the free surface at the centre of the vortex: each time the wave reaches the surface it causes a significant change in the surface level and hence the transit time can be determined fairly accurately. A typical set of measurements of the level of the surface is shown in figure 4. These results not only indicate the speed of the wave, but also give the value of z_0 which specifies the critical speed of infinitesimal waves. An interesting feature of the results of figure 4 is the decrease in the wave speed as the time increases, corresponding to a decrease in z_0.

The results of the measurements of the wave speeds are shown in figure 5, and the curves for the critical speed W_0, according to the two models (see (3.16) and (3.25)), are also shown. The measured wave speeds are about 6 % smaller than the critical speed predicted by the more realistic model. That the measured

† The best way the author found of observing the motions was to have a pH indicator (e.g. Thymol Blue) in the solution and then introduce one or two drops of sodium hydroxide at the centre of the vortex. This can be done conveniently at both the top and bottom of the container.

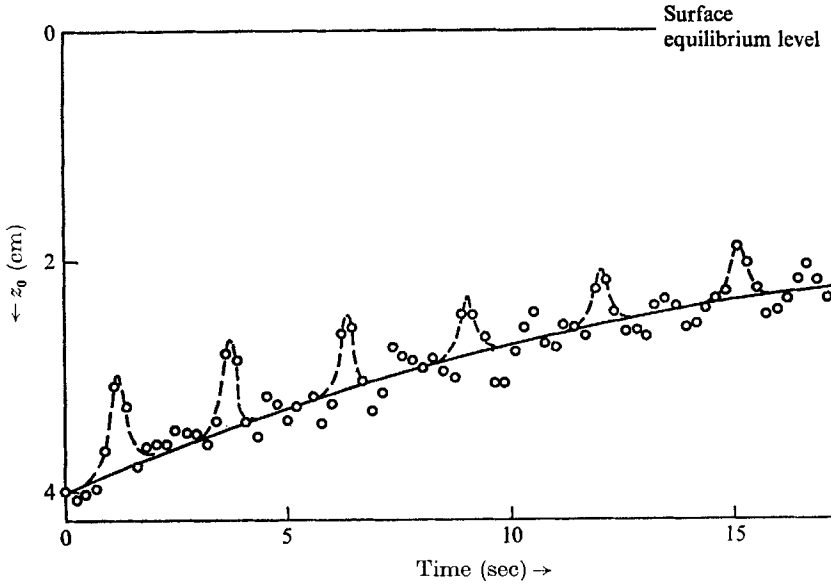

FIGURE 4. The depression of the free surface at the centre of the vortex, showing the presence of the solitary wave. The undisturbed depth of liquid in the container was 56·9 cm.

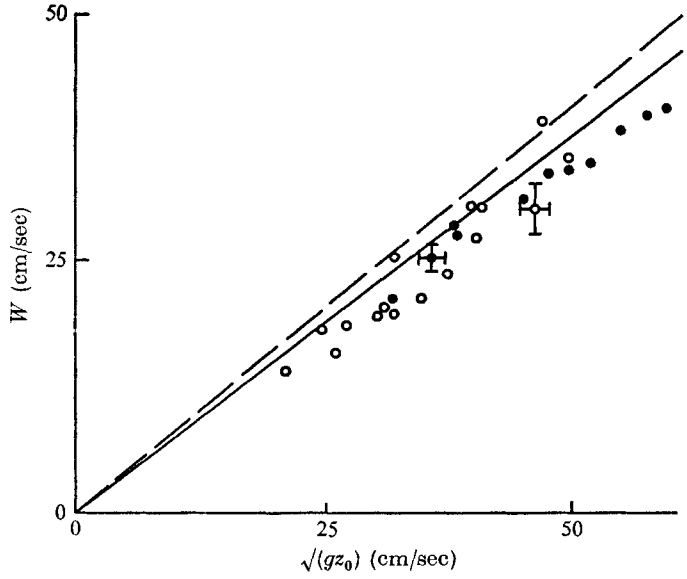

FIGURE 5. The velocity of the solitary wave in a fluid of large radial extent. The curves are the estimates of the critical speed of infinitesimal waves: — — —, Rankine-vortex model (equation (3.16)); ———, Burgers-vortex model (equation (3.25)).

wave speeds do not exceed the critical speeds is a little disquieting, but as there are a number of approximations involved in the interpretation of the experiment this discrepancy may not be as serious as it appears at first sight. For example, the speed of the wave has been determined from the time taken for the wave to travel a distance equal to twice the distance between the free surface at the centre of the vortex (when the wave is not near the surface) and the bottom of the container. The fact that the arrival of the wave changes the shape of the free surface suggests that the measurements shown in figure 5 underestimate the actual wave speeds.

Another source of error will arise from the finite radial dimension of the container. For the case of the Rankine-vortex model it is fairly easy to estimate the effect the container wall has on the critical speed. We assume that the primary velocity distribution is given by (3.6), but that the wall of the container is at $\eta = Y$, where $Y > \alpha$. It then remains to solve (3.7) in conjunction with (3.2) for extremely long ($k = 0$) sinusoidal waves, with the boundary conditions $\phi(0) = 0$ and $\phi(Y) = 0$. The solution of this eigenvalue problem is given by

$$J_1(s) + \mu s J_0(s) = 0, \tag{5.1}$$

where $s = 2\Omega\sqrt{(2\alpha)}/W$ and $\mu = (Y-\alpha)/2\alpha$. For large values of μs the zeros of (5.1) lie near the zeros of J_0 and it is easily shown that the critical speed is approximately

$$W_0 = \frac{2\Omega\sqrt{(2\alpha)}}{j_{0,1} + (\mu j_{0,1})^{-1}}. \tag{5.2}$$

In the present experiments $\mu \sim 5$, and hence the effect of the finite size of the container is to decrease the critical speed by about 8 % of that estimated in (3.11). On the other hand, the method used to estimate z_0 (namely the difference between the equilibrium level of the surface before the stirring and the surface level at the centre of the vortex) introduces a compensating error to the theoretical estimate of the critical speed. For the Rankine-vortex model the error may be found fairly easily, and when $\alpha/Y = 0{\cdot}1$ this method of measurement underestimates $\sqrt{(gz_0)}$ (and hence $\Omega\sqrt{\alpha}$) by 9 %. Thus it appears that these two sources of error very nearly balance each other.

Another possible source of error may arise from the reflecting properties of the wave (especially at the free surface) about which very little is known theoretically. To indicate that this mechanism or that some systematic error introduced during the measurement of the wave speed could account for the discrepancy shown in figure 5, further (slightly less accurate) measurements of wave speeds were made in different depths of liquid. The results of these measurements are given in figure 6, and summarized in table 1. (This rather complicated figure has been included here to indicate that the error may not be a constant function of the wave speed.) To summarize the measurements of figure 6 we have used the result of (3.25) that, to first order, $\sqrt{(gz_0)}/W$ is a constant ($= 1{\cdot}30$). Thus, for each of the depths of liquid used, the mean value and standard deviation of this ratio have been determined and are given in table 1.

The difference between any two of the mean values of $\sqrt{(gz_0)}/W$ (except for

the 40 and 45 cm pairing) is highly significant. It therefore appears that this source of error could easily account for the above-mentioned discrepancy in the wave speed.

Depth of liquid (cm)	Mean value of $\sqrt{(gz_0)}/W$	Standard deviation of $\sqrt{(gz_0)}/W$
60	1·369	0·130
45	1·691	0·175
40	1·726	0·185
30	1·861	0·283

TABLE 1

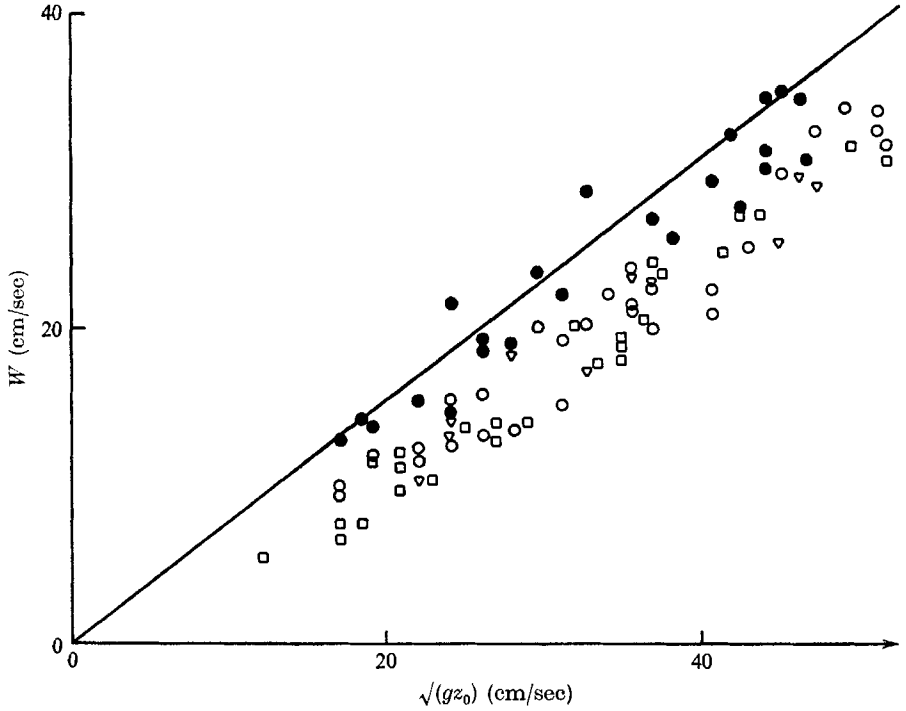

FIGURE 6. Estimates of the velocity of the solitary wave for various depths (D) of liquid. ●, D = 60 cm; ○, D = 45 cm; ▽, D = 40 cm; □, D = 30 cm. ———, $W = \sqrt{(gz_0)}/1{\cdot}30$.

6. Experiments in a long tube

The apparatus used for these experiments has been described in detail in a previous paper (Pritchard 1969). Briefly it consisted of a cylindrical tube of 5·1 cm diameter and 183 cm in length. The tube was mounted vertically and was (usually) rotated at speeds of about 2π radian/second. Thin platinum wires spanned the tube at three axial positions and were used as the cathode of an electrolytic cell. Dye traces were produced at these wires by local colour changes of the indicator Thymol Blue in response to an electric potential being applied

to the cell (see Baker 1966 for details of the method), and these dye traces were used to visualize the fluid motions. The movements of a dye trace were recorded on ciné film, and by employing a suitable arrangement of mirrors two of these traces could be recorded, side-by-side, on each frame of the film.

It was anticipated that solitary waves could be generated in this experiment in an analogous fashion to that used in open channels. A convenient way of making solitary waves in a channel is to create a 'mound' of liquid by displacing a paddle fairly vigorously along the channel for a short distance: a solitary wave usually emerges from the disturbance and propagates along the channel to large distances. If, however, attempts are made to generate a wave of depression in this manner, there results only a transient disturbance which rapidly disperses.

With regard to the present experiments Benjamin (1967*a*) has shown, for a circumferential velocity distribution of a similar kind to those encountered here, that the solitary wave is a wave of inward displacement. This is the type of motion produced by moving a body (e.g. a sphere) along the axis of rotation in the opposite direction to the direction of propagation of the wave. But, the presence of a body in the liquid during the spinning-up process gives rise to strong meridional flows as a result of the Ekman layers on the surface of the body; this meridional circulation not only affects the circumferential velocity distribution, but also complicates the flow visualization. Hence this technique is not a very desirable way of generating solitary waves. On the other hand, a wave of inward displacement may be generated by moving an annular body (viz. a body that covers the area of the tube between the radius a and the wall of the tube) in the same direction as the direction of propagation of the wave. Consequently, there is no need to introduce this body into the liquid until it is desired to generate the wave. For similar reasons it is more convenient to use the (conventional) solid body to generate waves of outward displacement, which we anticipate not to have a permanent form.

To produce a wave of large amplitude it was necessary to create a vigorous disturbance with the body, and this was most conveniently done by plunging it into the liquid by hand.† Using the annular body a wave would emerge out of the disturbance, travel completely down the tube, and be reflected at the other end. However, when attempts were made to generate waves of outward displacement, by plunging in the solid body, the resulting waves dispersed very rapidly. The wave shape was determined from ciné-film records by measuring the displacement of the particle on the axis, and from this measurement the velocity distribution (w) within the wave was computed. Some typical measurements of this kind are given in figure 7. These results provide very convincing evidence for the solitary wave: curve (A) is the velocity distribution of a wave form generated when the solid body was displaced in the opposite direction to the direction of propagation of the wave and is a wave of inward displacement;

† The annular body was a long hollow cylinder which neatly fitted in the tube and hence was guided by the walls of the tube as it was pushed along the axial direction. The solid body was also a long cylinder and covered the complementary area of the tube; it was fitted inside the annular body with its end protruding some distance below the end of the annular body and thus the solid body also was guided truly along the axis.

(*B*) is the result of plunging the solid body into the liquid thereby generating a wave of outward displacement. The curves (*C*) and (*D*) are the analogous results obtained with the annular body.†

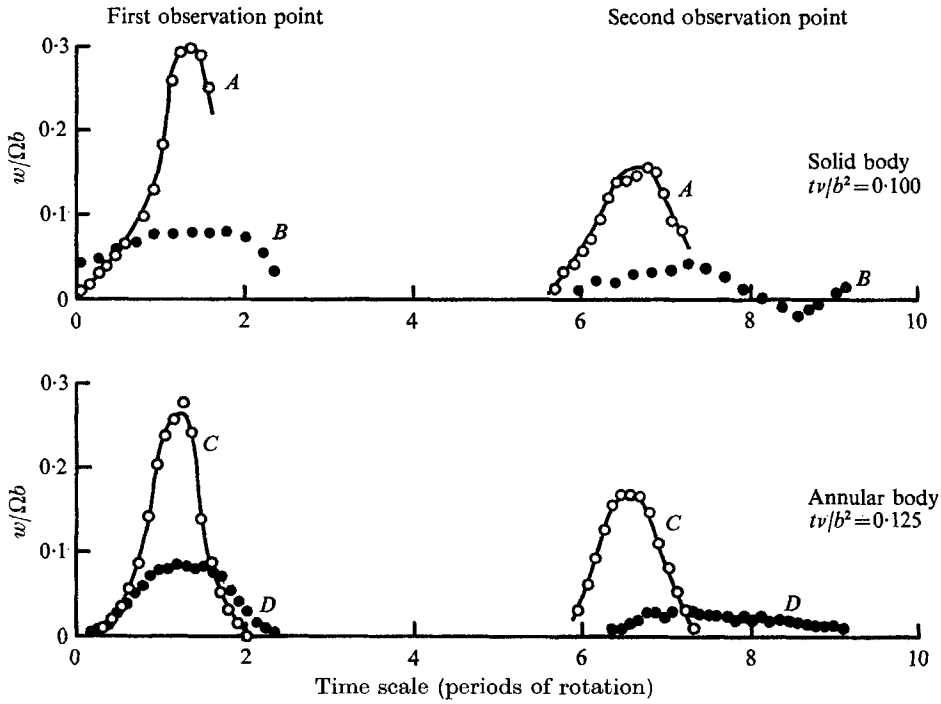

FIGURE 7. Two comparisons of a wave of elevation (●) with a wave of depression (○) for motions in a long cylindrical tube. The two observation points are separated by 15·5*b*. The waves were generated 18*b* above the first observation point.

An attempt has been made to measure the radial displacements associated with the solitary wave. The measurements were taken from a cylindrical sheet of dye formed from a platinum wire that stretched parallel to the axis. The results of this measurement are given in figure 8. Unfortunately, the passage of the wave

† It is evident from figure 7 that the amplitudes of the (solitary) waves decrease fairly rapidly as the wave travels along the tube: for example, for wave form (*C*), the ratio of the amplitudes at the two observation points is 0·65. This change of amplitude is attributed to viscous damping in boundary layers near the walls of the tube. A rough estimate of this damping has been made (see Pritchard 1968), following a similar calculation to that of Keulegan (1948); the calculations estimate that the amplitude of the wave is given by $A = A_0\, e^{-N(x/b)}$ after it has travelled a distance x along the tube. The constant N is given by $N = 3{\cdot}12\ (\nu/bL\Omega)^{\frac{1}{2}}$, where L is an effective length of the wave and ν is the kinematic viscosity of the fluid. For the purposes of this calculation the amplitude A was taken to be a constant within the wave. Applying this theory to wave form (*C*) the value obtained for A/A_0 was 0·64. While the agreement of this answer with the experimental value is most probably fortuitous, it does suggest that the observed change of amplitude can be attributed to viscous dissipation. Similar computations made on waves generated in uniformly rotating fluids, where a wave of permanent form does not exist, indicated that this viscous damping could *not* account *completely* for the change in amplitude of the wave form (cf. Pritchard 1968).

always caused the cylinder of dye to lose its axial symmetry, leaving it with a slightly elliptical cross section and thereby introducing a lot of scatter to the results. However, the measurements show that this is certainly a wave of inward displacement, and that a typical particle displacement at $r/b \sim 0{\cdot}5$, for these waves, is about 10 % of the tube radius. A wave of elevation, produced under the same conditions, gave a radial displacement of about $0{\cdot}045b$ at $r/b \sim 0{\cdot}5$.

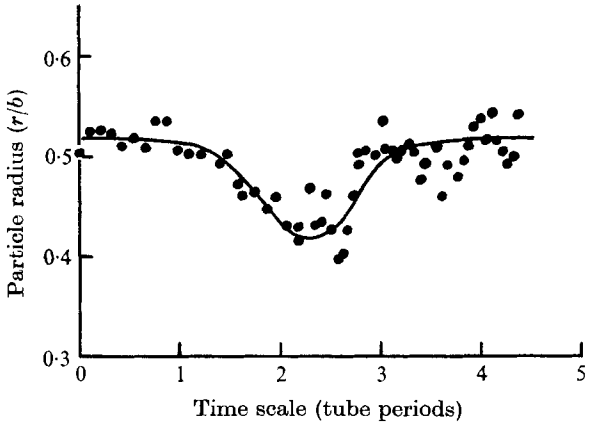

FIGURE 8. A measurement of the radial displacement associated with the solitary wave. The wave form was observed at $t\nu/b^2 = 0{\cdot}10$.

To compare the observed shapes of the solitary waves with the theoretical wave form (4.18) we must first estimate the amplitudes of the waves, which are specified by the departure of the wave speeds from the critical speed for infinitesimal waves. As indicated above the critical speed W_0 has been estimated from the theoretical velocity distribution (3.27) and the results of this calculation are given in figure 9. Also shown in figure 9 are some measurements of the wave speed W, which was determined from the time taken for the wave to travel between two observation points along the tube. The error in measuring these wave speeds is less than 2 %. However, in the time taken for the wave to travel between the two observation points the circumferential velocity distribution changed significantly and hence the theoretical velocity distribution (3.27) was computed for the mean value t had during the time the wave travelled between the two observation points.

When $t\nu/b^2$ is about 0·08 the circumferential velocity distribution is very nearly a parabolic function of the radius. Thus, in view of the approximations involved in the experiment, it seems reasonable to compare a wave form observed at an instant near $t\nu/b^2 = 0{\cdot}08$ with the theoretical solitary wave that would arise on the swirling flow in which V is proportional to r^2: for a distribution of this kind the theoretical wave shape may be found easily (see Benjamin 1967*a*).

A measurement of the displacement and velocity of a particle on the axis is shown in figure 10 for a wave generated at $t\nu/b^2 = 0{\cdot}092$. The theoretical wave form of figure 10 has been computed on the assumption that the wave is propagating into a parabolic distribution of circumferential velocity, and

that the critical speed W has the value given by the model distribution (3.27) at $t\nu/b^2 = 0{\cdot}092$. The agreement between the experimental results and the theory is thought to be remarkably good when the many approximations involved with

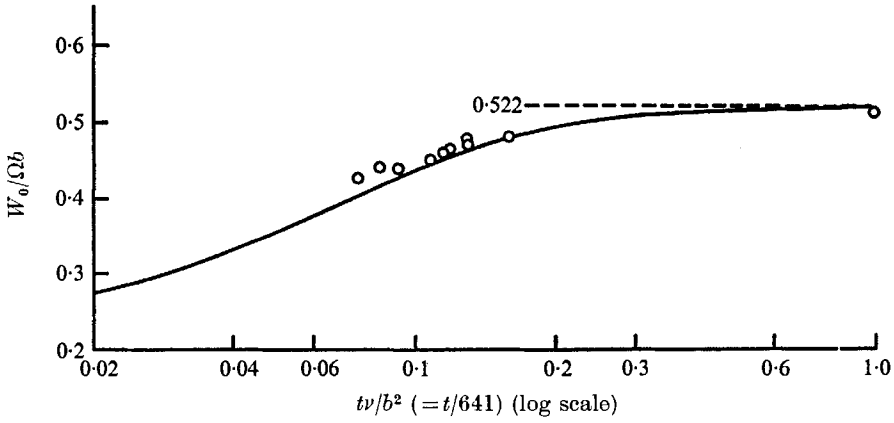

FIGURE 9. The critical speed for infinitesimal waves propagating in a circumferential velocity distribution of the form (3.27). The experimental points are velocities of solitary waves generated at the specified times after the beginning of the tube rotation.

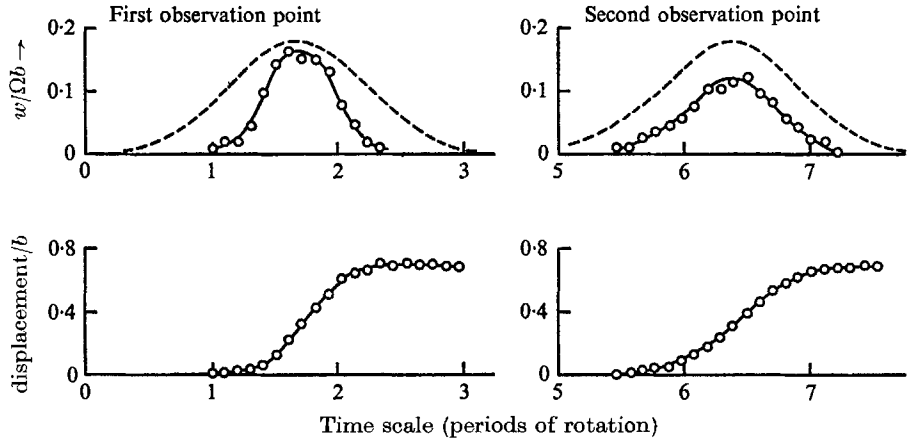

FIGURE 10. A solitary wave in a long cylinder of rotating liquid showing the displacement and velocity of particles on the axis at two positions along the tube separated by $16b$. The wave form was measured at $t\nu/b^2 \approx 0{\cdot}092$. W_0 (theoretical) = $0{\cdot}423\Omega b$; W(measured) = $0{\cdot}438\Omega b$. The dashed curve is the theoretical wave form from Benjamin (1967*a*) using these values of W and W_0, and assuming a parabolic distribution of the circumferential velocity. The wave was generated $18b$ above the first observation point.

the experiment are taken into account: the amplitude and length of the theoretical wave form depend crucially on the factor $(W - W_0)$, which is small, and we have already indicated there is some uncertainty in W_0. However, this comparison between the theory and the experimental results does suggest that the solitary wave may be a little shorter than is expected at the second stage of approximation.

This work was carried out at the Department of Applied Mathematics and Theoretical Physics, Cambridge. The author wishes to thank Dr T. B. Benjamin for his many suggestions and considerable help during the course of the work.

The author was supported by the Commonwealth Industrial Gases Ltd (Australia) to whom he is greatly indebted.

REFERENCES

BAKER, D. J. 1966 A technique for the precise measurement of small fluid velocities. *J. Fluid Mech.* **26**, 3.

BATCHELOR, G. K. 1967 *An Introduction to Fluid Dynamics.* Cambridge University Press

BENJAMIN, T. B. 1962 Theory of the vortex breakdown phenomenon. *J. Fluid Mech.* **14**, 593.

BENJAMIN, T. B. 1965 Significance of the vortex breakdown phenomenon. *Trans. Am. Soc. Mech. Engrs J. Basic. Engng*, **87**, 518.

BENJAMIN, T. B. 1967*a* Some developments in the theory of vortex breakdown. *J. Fluid Mech.* **28**, 65.

BENJAMIN, T. B. 1967*b* Internal waves of permanent form in fluids of great depth. *J. Fluid Mech.* **29**, 559.

BENJAMIN, T. B. & BARNARD, B. J. S. 1964 A study of the motion of a cavity in a rotating fluid. *J. Fluid Mech.* **19**, 193.

DAVIS, R. E. & ACRIVOS, A. 1967 Solitary internal waves in deep water. *J. Fluid Mech.* **29**, 593.

FRAENKEL, L. E. 1956 On the flow of rotating fluid past bodies in a pipe. *Proc. Roy. Soc.* A **233**, 506.

GRANGER, R. A. 1968 Speed of a surge in a bathtub vortex. *J. Fluid Mech.* **34**, 651.

HARVEY, J. K. 1962 Some observations of the vortex breakdown phenomenon. *J. Fluid Mech.* **14**, 585.

KEULEGAN, G. H. 1948 Gradual damping of solitary waves. *J. Res. Natn. Bureau of Standards*, **40**, 487.

LAMBOURNE, N. C. & BRYER, D. W. 1962 *Aero. Res. Coun. R & M.* no. 3282.

MAXWORTHY, T. 1966 At the I.U.T.A.M. Symposium on rotating fluid systems. See Bretherton, F. P., Carrier, G. F. & Longuet-Higgins, M. S. *J. Fluid Mech.* **26**, 393.

MAXWORTHY, T. 1968 The observed motion of a sphere through a short, rotating cylinder of fluid. *J. Fluid Mech.* **31**, 643.

PRITCHARD, W. G. 1968 A study of wave motions in rotating fluids. Ph.D. dissertation, University of Cambridge.

PRITCHARD, W. G. 1969 The motion generated by a body moving along the axis of a uniformly rotating fluid. *J. Fluid Mech.* **39**, 443.

TAYLOR, G. I. 1922 The motion of a sphere in a rotating liquid. *Proc. Roy. Soc.* A **102** 180.

TURNER, J. S. 1966 The constraints imposed on tornado-like vortices by the top and bottom boundary conditions. *J. Fluid Mech.* **25**, 377.